Preparation of microwave-assisted expired honey derived electrodes with excellent performance for supercapacitors

Xinting Yu[†a], Yuxin Zhu[†b],Yunqiang Zhang[*b], Mei Li[*b]

a Department of Science and Engineering Education, Shandong Open University, Jinan 250002, China

b School of Materials Science and Engineering, Qilu University of Technology (Shandong Academy of Sciences), Jinan, 250353, China.

*Corresponding authors: Yunqiang Zhang(yun_zhang@qlu.edu.cn)；Mei Li (lim@qlu.edu.cn);

Figures

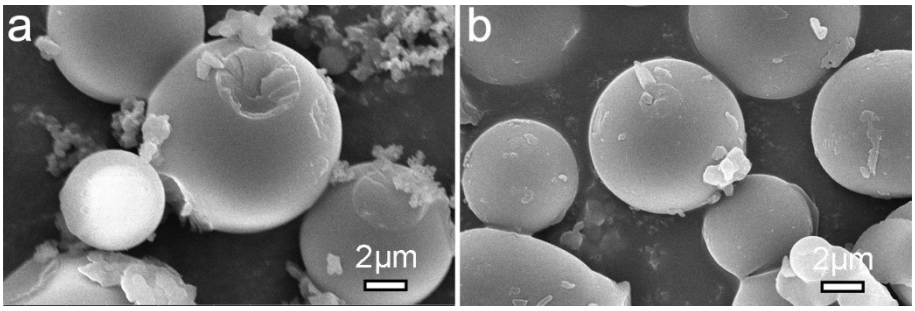

Fig. S1. SEM images of CHC and CMC samples before carbonization: (a) BH, (b) BM.

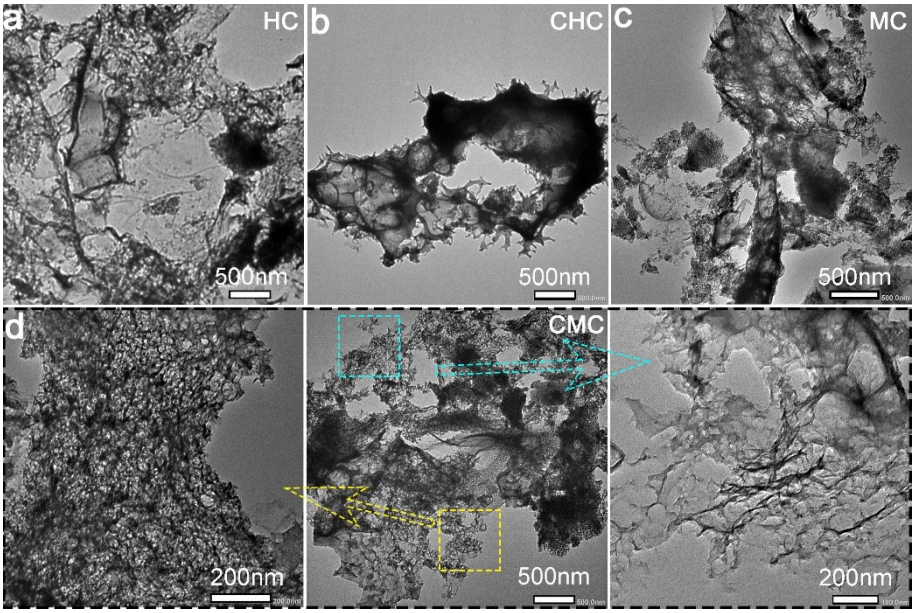

Fig. S2. TEM images in different magnification: (a) HC, (b) CHC, (c) MC, (d) CMC.

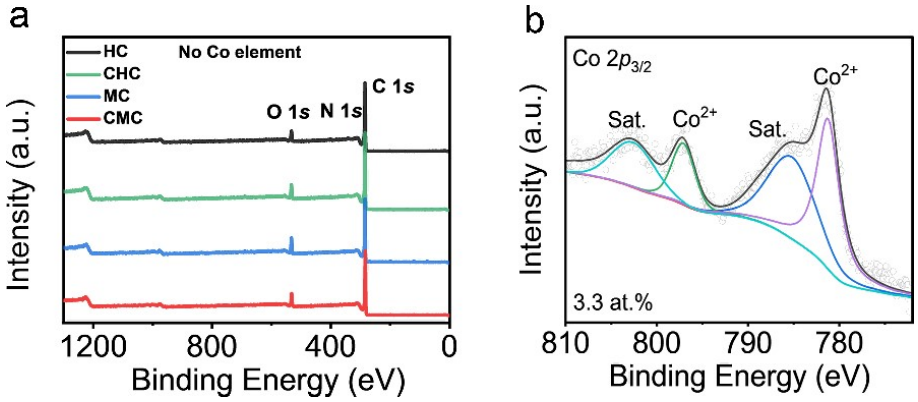

Fig. S3. (a) XPS survey spectrum of HC, CHC, MC and CMC. (b) Co 2p of

intermediate product after carbonization but before acid washing.

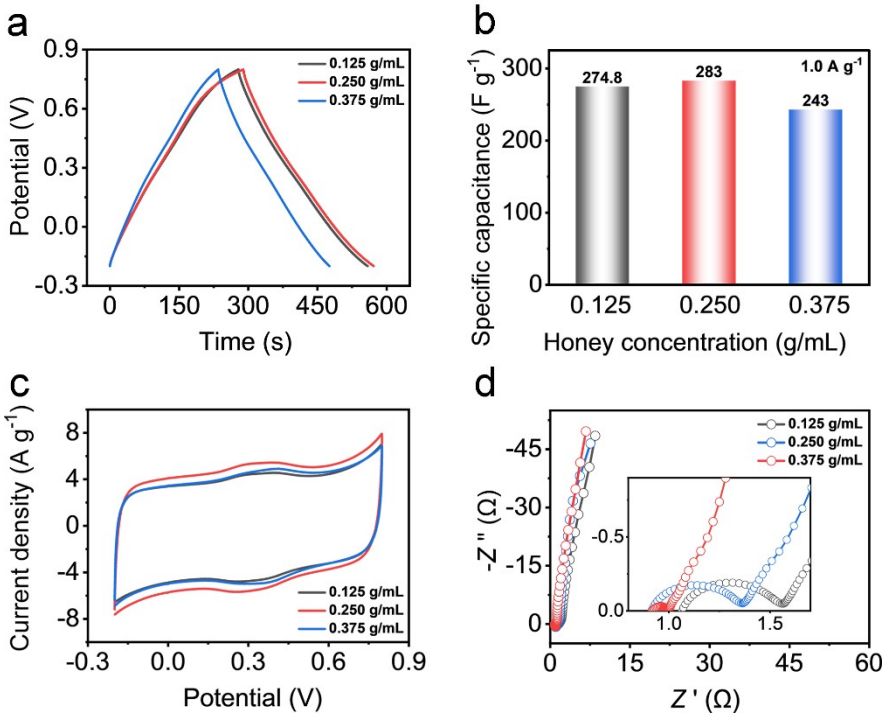

Fig. S4. Electrochemical performance of samples with different honey concentration under hydrothermal conditions: (a) GCD curves at 1.0 A g^{-1}, (b) the C_{sp} values at 1.0 A g^{-1}, (c) CV curves at 10 mV s^{-1}, (d) Nyquist plots.

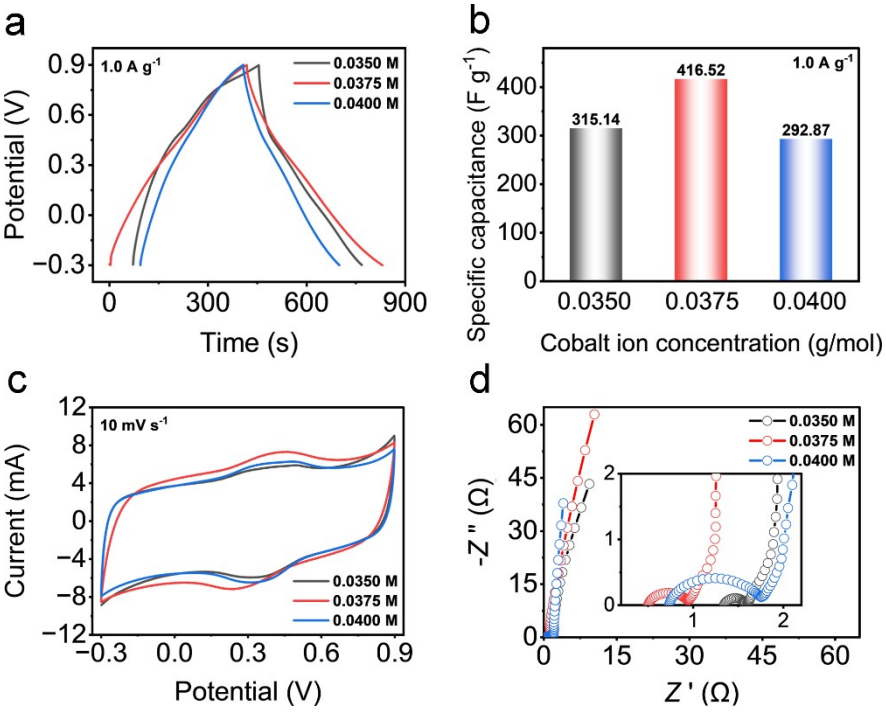

Fig. S5 Electrochemical performance of samples with different cobalt ion concentration under hydrothermal conditions: (a) GCD curves at 1.0 A g^{-1}, (b) the C_{sp}

values at 1.0 A g^{-1}, (c) CV curves at 10 mV s^{-1}, (d) Nyquist plots.

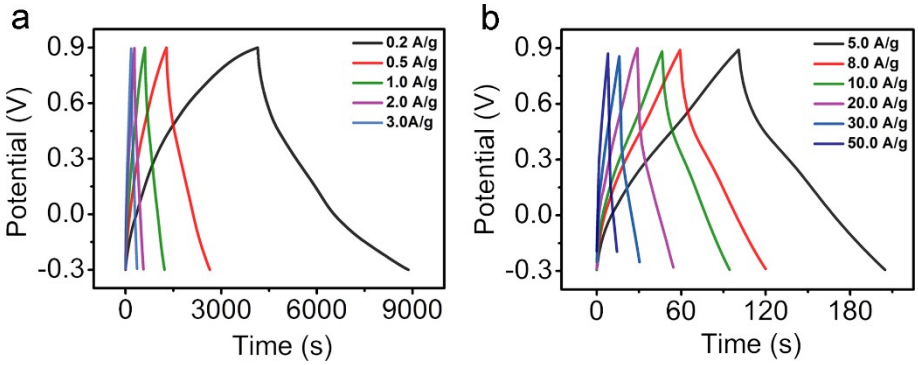

Fig. S6 GCD curves of CMC at (a) 0.2~3.0 A g^{-1}, (b) 5.0~50.0 A g^{-1}.

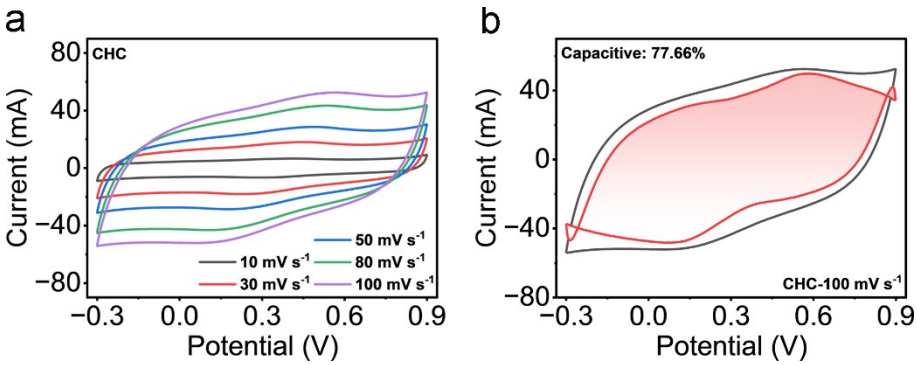

Fig. S7 CV curves at different scan rates of (a) CMC, (b) CHC and (c) pseudo-capacitance contribution of CHC at 100 mV s^{-1}.

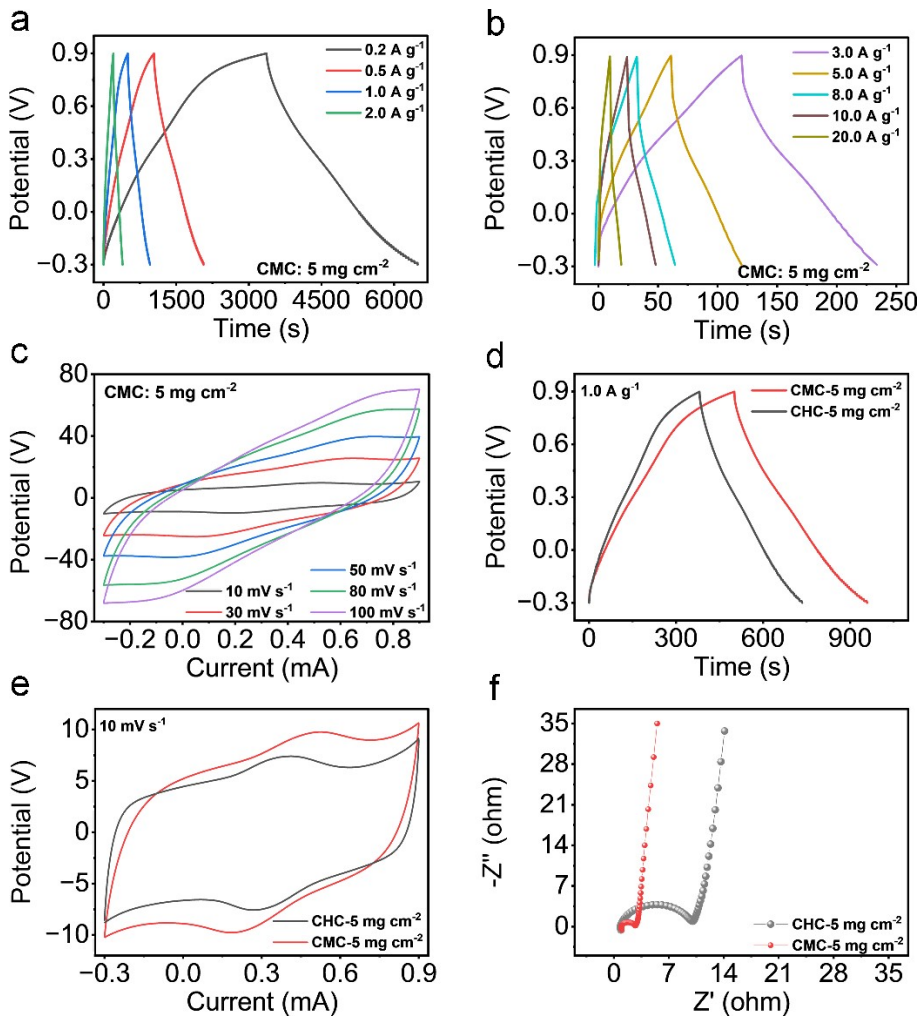

Fig.S8 GCD curves of CMC at the loading of 5 mg cm^{-2} under (a) 0.2~2.0 A g^{-1}, (b) 3.0~20.0 A g^{-1}, (c) CV curves at different scan rates, (d) GCD curves, (e) CV curves at 10 mV s^{-1}, (f) Nyquist plots of CMC and CHC.

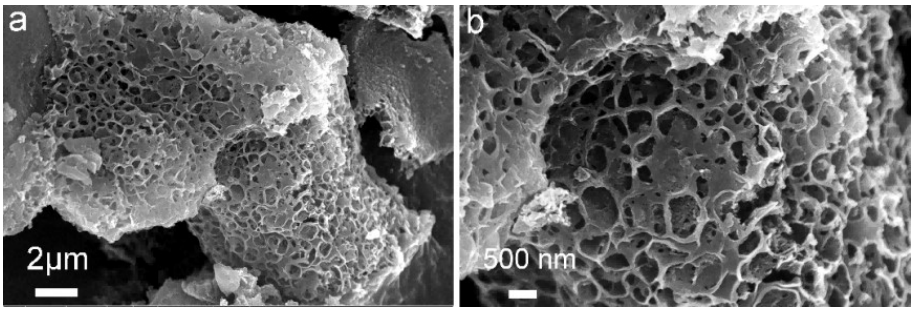

Fig. S9 SEM images of CMC after 15,000 charge-discharge cycles.

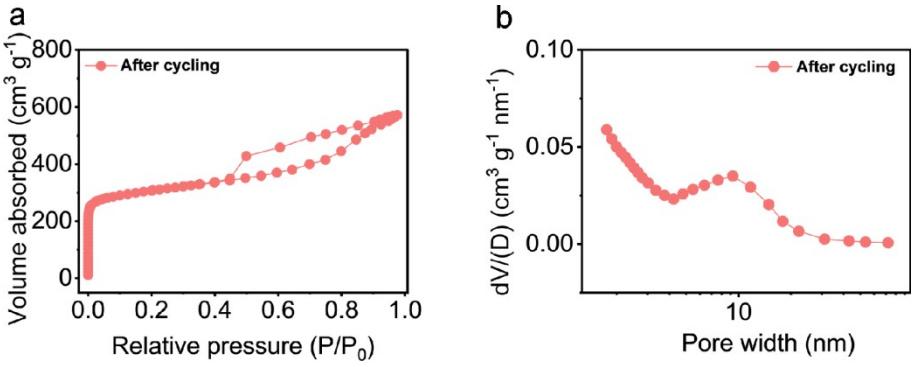

Fig. S10 Pore structural analysis of CMC after 15,000 charge-discharge cycles: (a) N_2 adsorption and desorption isotherms, (b) the corresponding pore size distributions.

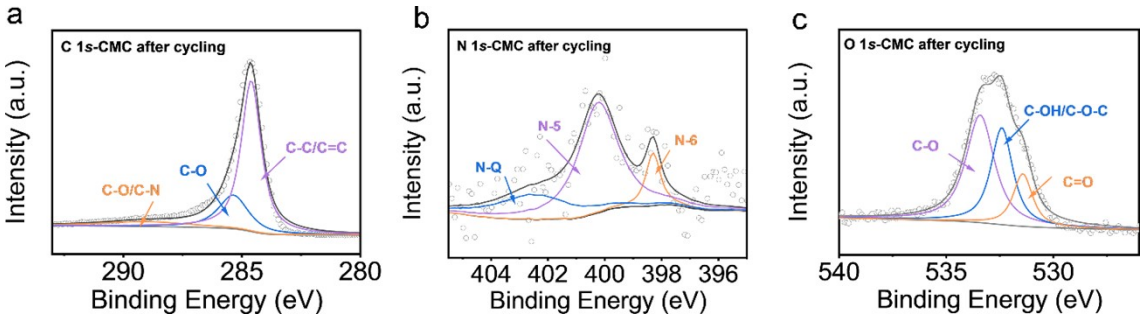

Fig. S11 High-resolution XPS scans for (a) C 1s, (b) N 1s and (c) O 1s of CMC after 15,000 charge-discharge cycles.

Tables

Table S1. Surface area and pore structure of HC, CHC, MC and CMC.

Samples	S_{BET}[a] ($m^2\ g^{-1}$)	S_{micro}[b] ($m^2\ g^{-1}$)	S_{meso}[c] ($m^2\ g^{-1}$)	V_{tot}[d] ($cm^3\ g^{-1}$)	V_{micro}[e] ($cm^3\ g^{-1}$)	Average pore size (nm)
HC	420.5	405.9	14.5	0.186	0.164	1.77
CHC	451.2	439.8	11.4	0.194	0.177	1.72
MC	1154.5	840.0	314.2	0.886	0.340	3.07
CMC	1404.6	1011.3	393.3	1.081	0.408	3.08

[a] The total surface area per unit mass or volume of as-prepared samples.

[b] The total surface area of micropores (pores with diameters less than 2 nanometers) per unit mass within a porous material.

[c] The total surface area occupied by mesopores (pores with diameters between 2 and 50 nanometers) per unit mass within a porous material.

[d] Total volume of all pores within a unit mass of material.

[e] The total volume occupied by micropores (pores smaller than 2 nanometers in diameter) per unit mass in porous materials.

Table S2. Elemental atomic ratio of samples.

Samples	Molar ratio of Co (wt%)
CMC	0.03

Table S3. Elemental atomic ratio of samples.

Samples	C (at%)	N (at%)	O (at%)
HC	90.71	1.38	7.91
CHC	90.78	0.51	8.71
MC	88.08	1.66	10.25
CMC	88.97	1.33	9.71

Table S4. Peak information points in detail of as-prepared samples.

Samples	HC		CHC		MC		CMC	
	Peaks (eV)	Proportion (at.%)	Peaks (eV)	Proportion (at.%)	Peaks (eV)	Proportion (%)	Peaks (eV)	Proportion (at.%)
C1s								
C-N/C-O	287.8	**21.18**	287.8	**19.67**	287.8	**18.78**	287.8	**14.31**
C=O	285.2	**38.01**	285.1	**29.53**	285.2	**39.82**	285.1	**30.59**
C-C/C=C	284.5	**40.81**	284.6	**50.80**	284.7	**41.40**	284.6	**55.10**
N1s								
N-Q	401.9	**35.01**	401.9	**60.15**	401.9	**29.65**	401.9	**64.88**
N-5	400.1	**42.79**	400.1	**30.60**	400.3	**55.07**	400.1	**22.58**
N-6	398.5	**22.20**	398.6	**9.25**	399	**15.28**	398.6	**12.54**
O1s								
C-O-C	533.1	**81.01**	533.2	**60.25**	533.2	**31.08**	533.1	**70.71**
C-O/C-OH	532.3	**12.03**	532.4	**24.07**	532.3	**42.40**	532.4	**14.49**
C=O	531.4	**6.96**	531.4	**15.68**	531.4	**26.52**	531.4	**14.80**

Table S5. Comparison of the electrochemical performance between the honey biochar prepared in this work and other biochar-based electrodes from the literature.

biochar materials	C_{sp} （F g^{-1}）	Cycle Stability (%)	Ref.
Cotton and catkin	367	92, 5000 cycles	[1]
hemp stems	220	96, 2000 cycles	[2]
Soybean oi	103	138, 1000 cycles	[3]
cow-ghee	266	99, 10,000 cycles	[4]
garlic peel	304 C/g	93, 10,000 cycles	[5]
loofah sponges	294	93.6, 30,000 cycles	[6]
corn straw powder	246.2	97.7, 10,000 cycles	[7]
Polypropylene packaging materials	403.67	95, 3,000 cycles	[8]
tea waste	334	91, 5,000 cycles	[9]
Ficus altissima branch wastes	378	78, 5000 cycles	[10]
Honey	780.2	96.7, 15,000 cycles	This work

Table S6. Surface area and pore structure of CMC after 15,000 charge-discharge cycles.

Samples	S_{BET} (m^2 g^{-1})	S_{micro} (m^2 g^{-1})	S_{meso} (m^2 g^{-1})	V_{tot} (cm^3 g^{-1})	V_{micro} (cm^3 g^{-1})	Average pore size (nm)
CMC after cycling	1296.3	956.1	340.2	0.965	0.351	2.80

Table S7. Peak information points in detail of CMC after 15,000 charge-discharge cycles.

Samples	CMC after cycling	
	Peaks (eV)	Proportion (at.%)
C1s (90.26 at.%)		
C-N/C-O	288.8	60.97
C=O	285.3	20.44
C-C/C=C	284.6	8.85
N1s (1.20 at.%)		
N-Q	402.7	0.84
N-5	400.2	0.12
N-6	398.3	0.24
O1s (8.54 at.%)		
C-O-C	533.4	4.22
C-O/C-OH	532.4	2.92
C=O	531.4	1.40

References:

[1] B. Chen, D. Wu, T. Wang, F. Yuan and D. Jia, *Chem. Eng. J.*, 2023, **462**, 142163.

[2] B. Tekin and Y. Topcu, *J. Energy Storage*, 2024, **77**, 109879.

[3] C. E. Sánchez-Rodriguez, J. J. Elisea-Espinoza, B. Portillo-Rodríguez and R. López-Sandoval, *Diamond Relat. Mater.*, 2024, **146**, 111213.

[4] S. Muduli, S. K. Pati and S. K. Martha, *Int. J. Energy Res.*, 2022, **46**, 14074-14087.

[5] R. J. Wesley, S. Vasanth, A. Durairaj, R. Justinabraham, C. Viswanathan, A. Obadiah and S. Vasanthkumar, *J. Energy Storage*, 2024, **91**, 112092.

[6] Y. Cheng, M. Chen, K. Xia, H. Li, G. Xu, L. Yang, Z. Zhao, P. Liu and L. Wang, *J. Power Sources*, 2024, **624**, 235523.

[7] Y. Zhao, H. Hu, F. Wang, Y. Yan, K. Ye, W. Zeng, K. Tang, A. Huang, S. Cai, L. Lan, L. Liu, W. Zhu, Y. Wang, Z. Yan, L. Qiao, W. Tang and M. Yan, *J. Power Sources*, 2025, **629**, 236016.

[8] S. Sekar, C. D. Venkatachalam, M. Sengottian and S. R. Ravichandran, *J. Energy Storage*, 2024, **104**, 114475.

[9] R. S. Karmur, D. Gogoi, M. R. Das and N. N. Ghosh, *RSC Adv.*, 2024, **14**, 27465-27474.

[10] Y. Wang, Y. Liu, X. Huang, G. He and K. Yan, *Chin. Chem. Lett.*, 2024, **35**, 109301.